

# Exponential decay properties of Wannier functions and related quantities

Lixin He and David Vanderbilt

*Department of Physics and Astronomy, Rutgers University, Piscataway, New Jersey 08855-0849*  
(January 19, 2001)

The spatial decay properties of Wannier functions and related quantities have been investigated using analytical and numerical methods. We find that the form of the decay is a power law times an exponential, with a particular power-law exponent that is universal for each kind of quantity. In one dimension we find an exponent of  $-3/4$  for Wannier functions,  $-1/2$  for the density matrix and for energy matrix elements, and  $-1/2$  or  $-3/2$  for different constructions of non-orthonormal Wannier-like functions.

PACS: 71.15.Ap, 71.20.-b, 71.15.-m

A growing interest in localized real-space descriptions of the electronic structure of solids has been motivated by the development of computationally efficient “linear-scaling” algorithms [1,2] and by the desirability of a local real-space mapping of chemical [3,4] and dielectric [5,6] properties. A primary avenue to such a description is the use of Wannier functions [7–9] (WFs), i.e., a set of localized wavefunctions  $w_{\mathbf{R}}(\mathbf{r})$  obtained from the Bloch functions  $\psi_{\mathbf{k}}(\mathbf{r})$  by a Fourier-like unitary transformation. A closely related approach is to represent the electronic structure in terms of the density matrix  $n(\mathbf{r}, \mathbf{r}')$ . It is thus not surprising to find considerable recent interest in the localization properties of the WFs [3] and of the density matrix [10,11].

In a classic 1959 paper, Kohn proved, for the case of a centrosymmetric crystal in one dimension (1D), that the WFs have an “exponential decay”  $w(x) \approx e^{-hx}$ , where  $h$  is the distance of a branch point from the real axis in the complex- $k$  plane [8]. More precisely,

$$\lim_{x \rightarrow \infty} w(x) e^{qx} = \begin{cases} 0, & q < h \\ \infty, & q > h \end{cases} \quad (1)$$

The density matrix has a similar decay  $n(x, x') \approx e^{-h|x-x'|}$ . The exponential decay of the WFs has since been proven for the general 1D [12] and single-band 3D [13] cases, and that of the density matrix (more precisely, of the band projection operator) has been proven in general [12]. The energy matrix elements  $E(R) = \langle w_R | H | w_0 \rangle$ , with  $w_R(x) = w(x - R)$  and  $R = la$  a lattice vector, are also expected to have a similar decay,  $E(R) \sim e^{-hR}$ .

The purpose of this Letter is to address two questions. First, Eq. (1) allows considerable freedom; in fact, it is consistent with

$$w(x) \approx x^{-\alpha} e^{-hx} \quad (2)$$

for *any* exponent  $\alpha$ , i.e., a decay which could be faster ( $\alpha > 0$ ) or slower ( $\alpha < 0$ ) than pure exponential. Does such a power-law prefactor exist, and if so, what is the exponent  $\alpha$ ? Second, it has long been understood that relaxation of the orthogonality constraint  $\langle w_0 | w_R \rangle = \delta_{0,R}$  can give “more localized” Wannier-like functions [14–16].

In what sense are these more localized – a larger  $h$ , or a larger  $\alpha$  for the same  $h$ , or only a smaller prefactor of the tail? We show that the power-law prefactors of Eq. (2) *do* exist, and that the various quantities have a common inverse decay length  $h$  but different exponents  $\alpha$ . In 1D we find that  $\alpha = 3/4$  for usual (orthonormal) WFs,  $\alpha = 1/2$  for  $n(x, x')$  and  $E(R)$ , and  $\alpha = 1/2$  or  $\alpha = 3/2$  for two different constructions of non-orthonormal Wannier-like functions (NWFs). The NWFs of superior decay ( $\sim x^{-3/2} e^{-hx}$ ) can be constructed by a projection method as duals to a set of trial functions. These results may have important implications for the design and implementation of efficient real-space electronic-structure algorithms.

We first review the central results of the pioneering work of Kohn [8], who considers a centrosymmetric potential of period  $a$  in 1D. The WFs are constructed as

$$w_n(x - R) = w_{nR}(x) = \frac{a}{2\pi} \int_{-\pi/a}^{\pi/a} e^{-ikR} \psi_{nk}(x) dk \quad (3)$$

with the phases of the Bloch functions  $\psi_{nk}$  chosen as in Sec. 6 of Ref. [8]. The exponential decay of the WFs is then governed by the positions of branch points in the “complex band structure”  $E_n(k)$  constructed by regarding complex  $E_n$  to be a function of complex  $k$  via analytic continuation from the real axis [8,9]. Specifically, there is a Riemann sheet  $E_n(k)$  for each band  $n$ , and the branch points  $k_n$  are the points at which the sheets are connected,  $E_n(k_n) = E_{n+1}(k_n)$ . These are located at

$$k_n = \begin{cases} \pi/a \pm ih_n, & n \text{ even} \\ \pm ih_n, & n \text{ odd} \end{cases} \quad (4)$$

and at translational image locations  $k_n^{(m)} = k_n + 2\pi m/a$  for integer  $m$ .  $E_n(k)$  and  $\psi_n(k)$  are thus analytic functions in the strip  $|\text{Im}(k)| < \bar{h}_n$  where  $\bar{h}_n = \min(h_{n-1}, h_n)$ . Kohn’s main result [8] is that the decay of the WF for the  $n$ ’th band is as  $w_n(x) \approx e^{-\bar{h}_n|x|}$  in the sense of Eq. (1). In what follows we restrict our attention to the bottom band ( $n=0$ ), for which  $\bar{h}_0 = h_0$  (henceforth just  $h$ ). The relevant branch point in the upper half-plane is  $k_0 = \pi/a + ih$  and the expected Wannier decay is  $w(x) \approx e^{-hx}$ .

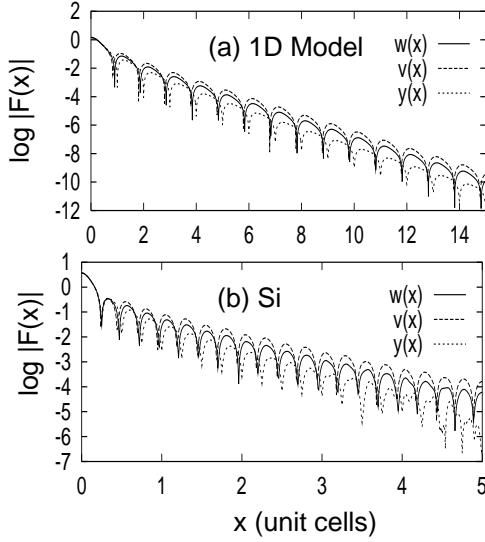


FIG. 1. Decay of normalized WFs  $w(x)$  and NWFs  $v(x)$  and  $y(x)$ . (a) 1D model (see text) with  $b=0.3$  and  $V_0=-10$ . (b) 3D Si plotted along the  $[110]$  direction.

To confirm this decay numerically, we first choose a simple 1D model Hamiltonian having a periodic potential  $U(x) = \sum_m V_{\text{at}}(x - ma)$  constructed as a sum of Gaussian “atomic” potentials  $V_{\text{at}}(x) = (V_0/b\sqrt{\pi})e^{-x^2/b^2}$ . Here  $a$  is the lattice constant and  $V_0$  and  $b$  control the depth and width of  $V_{\text{at}}$ . We choose units such that  $m=\hbar=e=1$  and keep  $a=1$  and  $V_0=-10$  fixed while adjusting  $b$  to vary the gap. The Bloch functions are computed on a mesh of 200  $k$  points by expanding in 401 plane waves and the WF at  $R=0$  is then constructed according to Eq. (3) using 128-bit arithmetic.

The resulting decay of the WF for  $b=0.3$  is shown as the solid line in Fig. 1(a). In this semilog plot, the approximate linearity of the peaks is consistent with the expected exponential decay, but there is a slight curvature that can be analyzed further. To do so, we first computed the  $E_n(k)$  along  $\pi/a + i\kappa$  for real  $\kappa$  and defined  $h$  to be the value of  $\kappa$  at which  $E_0 = E_1$ . For  $b=0.3$  we find  $h=1.28869$ . In Fig. 2(a) we then plot (diamonds)  $hx + \ln |w(x)|$  vs.  $\ln(x)$  for each peak of  $\ln |w(x)|$ . A pure exponential decay  $w(x) \approx e^{-hx}$  should yield a horizontal line in such a plot; instead, the data appears linear with a slope of  $-3/4$ , indicating that

$$w(x) \approx x^{-3/4} e^{-hx} . \quad (5)$$

A similar plot (not shown) for

$$E(R) = \langle w_R | H | w_0 \rangle = \frac{a}{2\pi} \int dk e^{ikR} E(k) . \quad (6)$$

suggests that  $E(R)$  shares the same inverse decay length  $h$  but has a different power-law exponent,

$$E(R) \approx R^{-3/2} e^{-hR} . \quad (7)$$

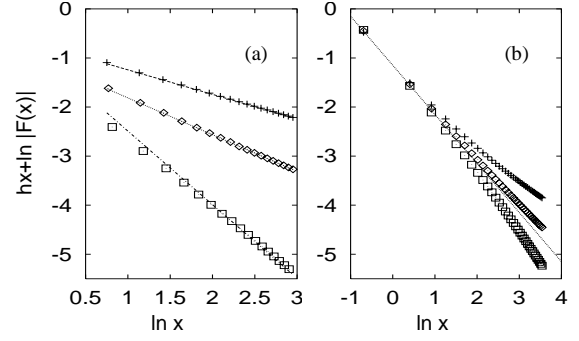


FIG. 2. (a) As in Fig. 1(a) but plotted so that slope reveals exponent  $-\alpha$  of Eq. (2). (b) Same for  $b=0.6$  (nearly-free electron case) showing crossover. Pluses, diamonds, and squares represent  $v$ ,  $w$ , and  $y$ , respectively.

Naturally  $h$  changes if the potential parameter  $b$  is varied, but we find that the power-law exponents of  $-3/4$  and  $-3/2$  do not. It thus appears that these exponents are a universal feature of electron bandstructures in 1D.

In order to gain an analytic understanding of this behavior, we consider first the simpler case of the energy-band Fourier transform  $E(R) \leftrightarrow E(k)$ . Kohn showed that the expansion of  $E(k)$  about  $k_0 = \pi/a + ih$  takes the form [8]

$$E(k) = E_0 + \gamma (k - k_0)^{1/2} + \dots \quad (8)$$

with higher terms of order  $(k - k_0)^1$ ,  $(k - k_0)^{3/2}$ , etc. The form of this expansion arises from the requirement that  $E(k)$  come back to itself if  $k$  traverses a closed path winding twice around  $k_0$ , consistent with the picture of two Riemann sheets touching at  $k_0$ .

Now there are well-known mathematical results that relate the behavior of a function near a branch point to the asymptotic decay of its Fourier transform [17]. The following lemma is useful here. Let  $f(k)$  be a periodic function  $f(k) = f(k + 2\pi/a)$  that has a leading behavior

$$f(k) = f_0 + \gamma [i(k - k_0)]^\beta \quad (9)$$

when expanded at the branch point  $k_0 = \pi/a + ih$ . Its Fourier series coefficients are given by

$$F(x) = \int_{C_0} f(k) e^{ikx} dk \quad (10)$$

at  $x = ma$  for integer  $m$ . As shown in Fig. 3, the contour  $C_0$  initially lies along the real axis. However,  $f(k) e^{ikx}$  is invariant under  $k \rightarrow k + 2\pi/a$ , and assuming that no other branch points or poles intervene, the contour can be deformed to become  $C_1$  as shown in Fig. 3. The exponential smallness of  $e^{ikx}$  for large  $x$  kills the integrals along the horizontal segments, and the dominant contribution to the  $C_1$  integral comes from the vicinity of  $k_0$ . Using the contour-integral definition of the Gamma function [18],

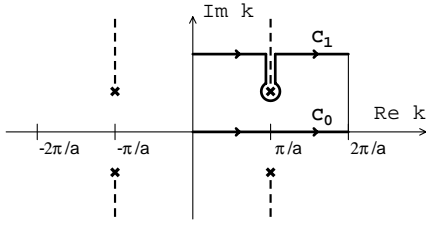


FIG. 3. Branch points ( $\times$ ), cuts (dashed lines), and integration contours ( $C_0$  and  $C_1$ ) in the complex- $k$  plane.

$$|F(x)| \simeq \gamma B(\beta) x^{-(1+\beta)} e^{-hx}, \quad (11)$$

where  $B_\beta = 2 \sin(\beta\pi) \Gamma(1 + \beta)$ .

Eq. (11) now allows us to understand the observed behavior of quantities such as  $E(R)$  and  $w(x)$ . For example, since  $E(k)$  in Eq. (8) has  $\beta = 1/2$ , we confirm that  $E(R) \approx R^{-\alpha} e^{-hR}$  with  $\alpha = 1 + \beta = 3/2$ . Similarly, to understand the decay of  $w(x)$ , we need to know the behavior of  $\psi_k(x)$  regarded as a function of  $k$  near the branch point  $k_0$ . Once again Kohn [8] provides the needed result  $\psi_k \approx (k - k_0)^{-1/4}$ . Sure enough,  $\beta = -1/4$  gives a decay  $w(x + R) \approx R^{-3/4} e^{-hR}$  for small  $x$  and  $R \gg a$ . In other words,  $w(x) \approx x^{-3/4} e^{-hx}$  for large  $x$ , as obtained numerically from Fig. 2(a).

We can summarize the information about both the  $k$ - and  $x$ -dependence of  $\psi_k(x)$  near the branch point as

$$\psi_k(x) = A_0(x) q^{-1/4} + A_1(x) q^{1/4} + \dots, \quad (12)$$

where  $q = i(k - k_0)$ . (All such terms have powers that are odd-integer multiples of  $1/4$ , consistent with  $\psi_k(x) \rightarrow -\psi_k(x)$  when traversing a closed path winding twice around  $k_0$ .)  $A_0(x)$  and  $A_1(x)$  are real functions obeying  $A_n(x + a) = e^{ik_0 a} A_n(x)$ .

The locality of the density matrix (i.e., the band projection operator) is also very important. For example, many linear-scaling algorithms are based on a direct solution for the density matrix [1,2,19]. We can write

$$n(x', x) = \frac{a}{2\pi} \int_{C_0} \psi_{-k}(x') \psi_k(x) dk \quad (13)$$

where, following Kohn [8], we have substituted  $\psi_k^*(x')$  by  $\psi_{-k}(x')$  in order that the integrand of Eq. (13) should remain analytic off the real axis. The behavior of  $\psi_{-k}(x)$  near the branch point is  $\psi_{-k}(x) \approx A_0(-x) [i(k - k_0)]^{-1/4}$ . The integrand of Eq. (13) then takes the form  $\psi_{-k}(x') \psi_k(x) \approx A_0(-x') A_0(x) [i(k - k_0)]^{-1/2}$ . Applying Eq. (11) yields  $n(0, x) \approx x^{-1/2} e^{-hx}$  for large  $x$ , and more generally,  $n(x', x) \approx (x - x')^{-1/2} e^{-h(x-x')}$  for  $x \gg x'$ . This  $\alpha = 1/2$  behavior of the decay has been confirmed from numerical plots (not shown) similar to Fig. 2(a).

We have so far shown that  $E(x)$ ,  $w(x)$ , and  $n(0, x)$  all have a decay of the form  $x^{-\alpha} e^{-hx}$  with a common  $h$  but with different (universal) exponents  $\alpha_E = 3/2$ ,  $\alpha_w = 3/4$ , and  $\alpha_n = 1/2$ . The energy matrix elements thus have the fastest decay, and the density matrix the slowest.

One may next ask whether it is possible to find non-orthonormal Wannier-like functions (NWFs) with a faster decay than those of the orthonormal WFs  $w(x)$  [14–16]. We explore this question in the context of band-projection methods [20–22]. We find that a naive application of the projection technique actually generates NWFs with a *slower* decay, while a modified “dual construction” approach *does* give improvement as measured by the exponent  $\alpha$ .

The basic idea of the projection technique is to start with a trial function  $t(x)$  and generate a Wannier-like function  $v(x)$  by acting with the band-projection operator  $\hat{P} = \sum_k |\psi_k\rangle \langle \psi_k|$ , i.e.,  $|v_R\rangle = \hat{P} |t_R\rangle$ . Here  $|t_R\rangle$  corresponds to the translational image  $t(x - R)$  of  $t(x)$  in cell  $R = na$ , and similarly for  $|v_R\rangle$ . The trial functions can be Gaussian functions, atomic or molecular orbitals, etc. The  $|v_R\rangle$  are NWFs having overlap  $S_{0R} = \langle v_0 | v_R \rangle = \langle t_0 | \hat{P} | t_R \rangle$ . Numerical investigations on C and Si by Stephan and Drabold indicated that the projected functions  $v(x)$  are *not* more localized than the true WFs  $w(x)$  [22]. This should not be surprising; introduction of NWFs may give flexibility to generate more localized orbitals, but this flexibility needs to be used to advantage. To do so, we introduce *dual* functions  $y(x)$  defined via  $|y_0\rangle = \sum_R (S^{-1})_{0R} |v_R\rangle$ , so that  $\langle y_0 | v_R \rangle = \delta_{0R}$  and also  $\langle y_0 | t_R \rangle = \delta_{0R}$ . This latter equation means that  $y(x)$  is orthogonal to the trial function at every site except  $R=0$ , suggesting that  $y(x)$  may be especially well localized.

Numerical tests of the decay of (normalized versions of)  $v(x)$  and  $y(x)$  are shown as dashed and dotted curves respectively in Figs. 1(a) and 2(a). The trial function used is a  $\delta$ -function on the atomic site, but use of other narrow trial functions gives similar results. It clearly appears that  $\alpha = 1/2$  and  $3/2$  for  $v(x)$  and  $y(x)$  respectively, to be compared with  $\alpha = 3/4$  for  $w(x)$ . Thus, the simple projected functions  $v(x)$  actually have a *slower* decay than the WFs  $w(x)$ , but the duals  $y(x)$  have a much faster decay than either of them.

These results can be explained by the complex analysis of the Bloch-like functions  $v_k(x)$  and  $y_k(x)$  that are related to  $v(x)$  and  $y(x)$  in the same way that  $\psi_k(x)$  is related to  $w(x)$ . Defining

$$\eta(k) = \int_{-\infty}^{\infty} \psi_{-k}(x) t(x) dx, \quad (14)$$

it follows from  $|v_k\rangle = |\psi_k\rangle \langle \psi_k | t \rangle$  that  $|v_k\rangle = \eta_k |\psi_k\rangle$ . Also the Fourier transform of  $S(0, R)$  can be seen to be  $S(k) = \eta^2(k)$ , so that  $|y_k\rangle = |\psi_k\rangle / \eta(k)$ . In the vicinity of  $k_0$  we have

$$\eta(k) = \eta_0 [i(k - k_0)]^{-1/4} + \eta_1 [i(k - k_0)]^{1/4} + \dots \quad (15)$$

where  $\eta_n = \int_{-\infty}^{\infty} A_n(-x) t(x) dx$ . Moreover,

$$\begin{aligned} v_k(x) &= \eta_0 A_0(x) q^{-1/2} + \dots, \\ w_k(x) &= A_0(x) q^{-1/4} + \dots, \\ y_k(x) &= \frac{1}{\eta_0} \left\{ A_0(x) + \tilde{A}_1(x) q^{1/2} + \dots \right\}, \end{aligned} \quad (16)$$

where  $q = i(k - k_0)$  and  $\tilde{A}_1(x) = A_1(x) - (\eta_1/\eta_0) A_0(x)$ . The leading term in  $y_k(x)$  gives no singularity, so the real-space decay is determined by the behavior of the next term for which  $\alpha = \beta + 1 = 3/2$ . To be explicit, we can define  $\mathcal{A}_n(x) = A_n(x) e^{hx}$  so that  $\mathcal{A}$  is anti-periodic,  $\mathcal{A}(x + a) = -\mathcal{A}(x)$ , and for large  $x$  we find

$$\begin{aligned} w(x) &\simeq B_{-1/4} \mathcal{A}_0(x) x^{-3/4} e^{-hx} , \\ v(x) &\simeq B_{-1/2} \eta_0 \mathcal{A}_0(x) x^{-1/2} e^{-hx} , \\ y(x) &\simeq (B_{1/2}/\eta_0) \tilde{\mathcal{A}}_1(x) x^{-3/2} e^{-hx} . \end{aligned} \quad (17)$$

The above conclusions regarding  $y(x)$  rely on the absence of zeros of  $\eta(k)$  inside the strip  $-h < \text{Im}(k) < h$ . If such zeros exist,  $y_k(x) = \psi_k(x)/\eta_k$  may have new singularities and  $y(x)$  will then have poor decay compared to other NWFs. We find that this problem does not arise when using  $t(x) = \delta(x)$  or a narrow Gaussian, but can be triggered by use of a too-wide Gaussian for  $t$ .

In view of  $n(x', x) = \sum_i w_i(x') w_i(x)$  it may appear surprising that  $n(x', x)$  decays more slowly than  $w(x)$  ( $\alpha_n=1/2$  vs.  $\alpha_w=3/4$ ). The representation of  $n$  via  $w$  thus has some advantages. Better yet, perhaps, one can represent  $n(x', x) = \sum_{ij} S_{ij} y_i(x') y_j(x)$ . Here the slow decay has been transferred to a simple matrix quantity ( $\alpha_S=1/2$ ) but the NWFs decay very quickly ( $\alpha_y=3/2$ ).

Is it possible to find a NWF with an even faster decay than  $x^{-3/2} e^{-hx}$ ? Yes; define a new NWF  $z_k = f(k) y_k$  where  $f(k)$  is analytic in the strip  $|\text{Im}(k)| < h$  and has simple zeros at the branch points  $(2n+1)\pi \pm ih$ . The function  $f(k) = 1 + \cos(ka)/\cosh(ha)$  is a good candidate [23]. Then the leading singularity of  $z_k$  is as  $(k - k_0)^{3/2}$ , and we expect  $z(x) \sim x^{-5/2} e^{-hx}$ . We have confirmed numerically that this works. However, since the multiplication by  $f(k)$  in  $k$ -space corresponds to a convolution in real space, the resulting  $z(x)$  is actually *broader* than  $y(x)$  or  $w(x)$  by almost any other measure (e.g., second moments [3]). Thus, this strategy may be counterproductive in practice.

Before leaving the 1D case, we make two brief comments. First, the extension to the case of non-centrosymmetric potentials in 1D is not difficult, and the results (including values of the  $\alpha$  exponents) are unchanged. Second, there is an apparent paradox concerning the nearly-free electron limit. For free electrons the occupied portion of the band gives  $w(x) \sim \sin(k_F x)/k_F x$ , i.e.,  $\sim x^{-1}$ . One may expect this to go over to  $\sim x^{-1} e^{-hx}$  in the nearly-free case, but this would be inconsistent with our general result  $\alpha = 3/4$ . Actually we find there is a crossover behavior, as shown in Fig. 2(b), with  $\alpha=1$  behavior for  $x \ll x_c$  and  $\alpha=3/4$  in the true large- $x$  tail. The crossover distance  $x_c$  increases as the gap decreases; as the gap closes,  $x_c \rightarrow \infty$  and  $h \rightarrow 0$ .

Before concluding, we briefly discuss the 3D case. Here the 6-dimensional space of complex  $(k_x, k_y, k_z)$  makes the formal analysis difficult. We have carried out a numerical calculation of WFs and NWFs for Si using an empirical-pseudopotential scheme starting from four bond-centered trial functions. The results are plotted in Fig. 1(b). Plots

of  $hx + \ln|F(x)|$  vs.  $\ln(x)$  (not shown) again show linear behavior, with slopes that appear consistent with the 1D values of  $\alpha = 3/4, 1/2$ , and  $3/2$  for  $w, v$ , and  $y$ , respectively. However, in this case we cannot afford to go to very large  $x$  values, and we suspect that there may be a crossover to larger  $\alpha$  values in the far tails. We leave this as a question for future investigations.

To conclude, we find that in 1D the asymptotic behavior of WFs and related quantities can all be expressed as  $x^{-\alpha} e^{-hx}$  with a common  $h$ , and with exponents  $\alpha$  that take on universal rational values depending on the type of singularity of the relevant function at the branch points in the complex- $k$  plane. It is surprising that this behavior has gone unnoticed since Kohn's seminal 1959 paper. The consequences for linear-scaling calculations, and localized real-space representations of electron structure more generally, remain to be fully explored.

This work was supported by NSF grant DMR-9981193.

- 
- [1] G. Galli, Curr. Opin. Sol. State Mater. Sci. **1**, 864 (1996).
  - [2] S. Goedecker, Rev. Mod. Phys. **71**, 1085 (1999).
  - [3] N. Marzari and D. Vanderbilt, Phys. Rev. B **56**, 12847 (1997).
  - [4] P.L. Silvestrelli, N. Marzari, D. Vanderbilt, and M. Parrinello, Solid State Commun. **107**, 7 (1998).
  - [5] I. Souza, R.M. Martin, N. Marzari, X. Zhao, and D. Vanderbilt, Phys. Rev. B **62**, 15505 (2000).
  - [6] P.L. Silvestrelli and M. Parrinello, Phys. Rev. Lett. **82**, 3308 (1999); J. Chem. Phys. **111**, 3572 (1999).
  - [7] G.H. Wannier, Phys. Rev. **52**, 191 (1937).
  - [8] W. Kohn, Phys. Rev. **115**, 809 (1959).
  - [9] E.I. Blount, Solid State Physics **13**, 305 (1962).
  - [10] S. Goedecker, Phys. Rev. B **58**, 3501 (1998).
  - [11] S. Ismail-Beigi and T.A. Arias, Phys. Rev. Lett. **82**, 2127 (1999).
  - [12] J. des Cloizeaux, Phys. Rev. **135**, A685 (1964).
  - [13] G. Nenciu, Commun. Math. Phys. **91**, 81 (1983).
  - [14] P.W. Anderson, Phys. Rev. Lett. **21**, 13 (1968).
  - [15] D.W. Bullett, J. Phys. C **8**, 2695 (1975).
  - [16] G. Galli and M. Parrinello, Phys. Rev. Lett. **69**, 3547 (1992).
  - [17] See, e.g., F.W.J. Olver, *Asymptotic and Special Functions* (A.K. Peters, Wellesley, MA, 1997), Sec. 3.12.
  - [18] I.S. Gradshteyn and I.M. Ryzhik, *Tables of Integrals, Series, and Products* (Academic Press, New York, 1980), 8.310.2.
  - [19] X.-P. Li, R.W. Nunes, and D. Vanderbilt, Phys. Rev. B **47**, 10891 (1993).
  - [20] J. des Cloizeaux, Phys. Rev. **135**, A698 (1964).
  - [21] S. Goedecker and L. Colombo, Phys. Rev. Lett. **73**, 122 (1994); S. Goedecker, J. Comp. Phys. **118**, 261 (1995).
  - [22] U. Stephan and D.A. Drabold, Phys. Rev. B **57**, 6391 (1998).
  - [23] Alternatively, the overlap  $S(k)$  itself can be used for this purpose via  $f(k) = S(k)^{-2}$ . This may be useful since one may not know the branch-point locations in advance.